Methods for Model-Aided In-Line Measurement and Control of Cross-Sections in Wire Rod and Bar Mills


Authors

Christian Overhagen (left)
University of Duisburg-Essen, Institute for Technology of Metals, Metal Forming Group, Assistant Professor, Duisburg, Germany
christian.overhagen@uni-due.de

Rolf Braun (right)
University of Duisburg-Essen, Institute for Technology of Metals, Metal Forming Group, Scientific Associate, Duisburg, Germany
rolf.braun@uni-due.de

In a research project, the Metal Forming Group of the University of Duisburg-Essen (UDE) collaborated with academic and industrial partners in Germany to develop sensors for an on-line measurement of material velocity and cross-section as well as control models for the rolling process of wire rod and bars. UDE provided a process model to assess the influencing parameters on the section precision. A technique was found to segregate height- from width-influencing parameters from measured cross-sectional area and actual roll gap. With this technology, rules for control of the rolling process to achieve close tolerances were obtained. Additionally, rolling trials on a laboratory rolling mill were carried out using a typical round-oval-round pass sequence for validation of the model. This article shows how a control of section tolerances is possible using the developed sensors and models.

In the hot rolling of wire rod, bars and other long products in continuous rolling mills, the sectional deviations along a rolled material strand are affected by temperature and size.[1] To ensure a stable rolling process with constant product quality, it is therefore necessary to control the rolling process. It can be observed that there is a coupling between the rolling stand and tools (i.e., the rolls) and the rolled material through the roll force. The roll force is strongly dependent on the deformation in the rolling pass, but in turn affects the roll gap and therefore the height of the rolled material. Different from flat rolling processes, in section rolling the lateral spread plays an important role in the section formation and cannot be neglected. The spread is also influenced by a variation of section height. Therefore, the cross-section of the rolled material is distorted in both height and width directions by elastic deformation of the rolling stands and tools. Other important influences are interstand tension stresses that arise in the rolled material between the stand positions. It is well known from rolling theory that roll force and torque are affected by tension stresses, but there is another direct influence of the interstand tensions on the spreading behavior of the rolling process. Therefore, the whole influence chain described here is affected further by acting interstand tensions.

These effects lead to the circumstance that a control of the rolling process for long products is much more complicated than that of the flat rolling process since the lateral spread must be considered in the analysis. In the joint project PIREF, the Metal Forming Group of University Duisburg-Essen (UDE) collaborated with the measurement technology group of the University of Applied Sciences Ruhr-West (HRW), the control theory group of the University of Siegen (USI) as well as the sensor manufacturing company EMG Automation GmbH (EMG) and SMS group GmbH. The main task of the UDE work group was to provide a process model for the rolling processes to achieve a mathematical description of all important metal forming effects and interdependencies. This process model was later implemented in the control models developed by USI. To enable process control during

rolling, cross-section sensors developed by the HRW were used (so-called QFM sensors) which are suited for an in-line use during the rolling process. With help of these sensors, the cross-section of the rolled strand could be measured during the rolling process at key positions in the rolling mill layout.

A Roll Gap Model for Bar Mills

For the process model, it is important to calculate roll force and torque as well as being able to predict the section shape, which is influenced by elastic rolling stand deformation as well as interstand tensions. The model follows the common philosophy that a rolling pass with section geometries is transferred into a geometrically similar flat rolling pass, for which the well-known theories of flat rolling can be applied. For the stress distribution, von Karman's differential equation is used:

$$\frac{d\left(\sigma_x h\right)}{d\alpha} = 2R\left(\sigma_N \sin\alpha - \tau_F \cos\alpha\right) \qquad \text{(Eq. 1)}$$

The solution of this differential equation requires further introduction of a suitable yielding criterion and a friction law. By making use of Tresca's criterion of yielding for the two possible friction laws of slipping and sticking friction, Alexander's rolling theory can be used to write out two ordinary differential equations for the normal stress:[3]

$$\frac{d\sigma_N}{d\alpha} = \frac{\left(\frac{2R'}{h} k_f \sin\alpha + \frac{dk_f}{d\alpha}\right)}{1 \mp \mu\tan\alpha} \sigma_N(\alpha) \pm \frac{\left(\frac{\mu}{\cos\alpha}\frac{2R'}{h} + \frac{1}{\cos\alpha}\right)}{1 \mp \mu\tan\alpha} \text{ for slipping fraction} \qquad \text{(Eq. 2)}$$

$$\frac{d\sigma_N}{d\alpha} = k_f \left\{\frac{2R'}{h}\sin\alpha\left(1+\frac{1}{2}\tan\alpha\right) - \left(\frac{R'}{h}\cos\alpha + \frac{1}{2\cos\alpha}\right)\right\} + \left(1+\frac{1}{2}\tan\alpha\right)\frac{dk_f}{d\alpha} \text{ for sticking fraction} \qquad \text{(Eq. 3)}$$

For each position in the roll gap, the right friction law is chosen out of these two possibilities, from the criterion which one does not override the shear flow stress as the maximum possible plastic shear stress.

Finally, the following equations can be written out to calculate the roll force:

$$F = b\left\{\begin{array}{l} \int_0^{\alpha_0} \sigma_N(\alpha)\cos\left(\alpha - \frac{\alpha_0}{2}\right)d\alpha + \\ R'\int_{\alpha_F}^{\alpha_0} \tau_F(\alpha)\sin\left(\alpha - \frac{\alpha_0}{2}\right)d\alpha - \\ R'\int_0^{\alpha_F} \tau(\alpha)\sin\left(\alpha - \frac{\alpha_0}{2}\right)d\alpha \end{array}\right\} \qquad \text{(Eq. 4)}$$

In these equations, the flattened roll radius R' is given in terms of Hitchcock's theory of roll flattening according to Reference 4:

$$R' = R\left(1 + \frac{F}{b_m}\frac{C}{\Delta h}\right) \text{ with } C = \frac{16}{\pi}\cdot\frac{1-\nu^2}{E} \qquad \text{(Eq. 5)}$$

where

b_m = the width of the rolled material and
C = a characteristic figure describing the elastic surface flexibility of the roll material.

The rolling force as calculated by Eq. 4 provides the basis for an assessment of the elastic deformations of the rolling stand, which influences both height and width of the rolled section. The elastic deformation in height direction can be found from the Gagemeter equation with:

$$h_1 = s_0 + \frac{F}{C_S} \qquad \text{(Eq. 6)}$$

where

C_S = the mechanical rigidity of the rolling stand in kN/mm,
s_0 = the roll gap present at a zero roll force and
h_1 = the thickness of the rolled product at the roll gap exit.

To calculate the spread of a section pass, Lendl's equivalent rectangular pass method[5] and the spreading model according to Marini as discussed by Mauk

and Kopp are used.[2] The Marini model is also suitable to calculate the internal local spreading contour in each pass.

Fig. 1 shows a typical round-to-oval pass, where the entry round section is plotted over the oval groove. The areas of direct contact are identified as A_{0L} and A_{1L}. Note that these areas are smaller than the true cross-sectional areas A_0 and A_1 of the round and oval section.

The distance of the intersection points between groove and entry section is called the cut point distance b_L. To enable calculations of the spreading behavior, the equivalent heights of the section passes can be defined according to:

Figure 1

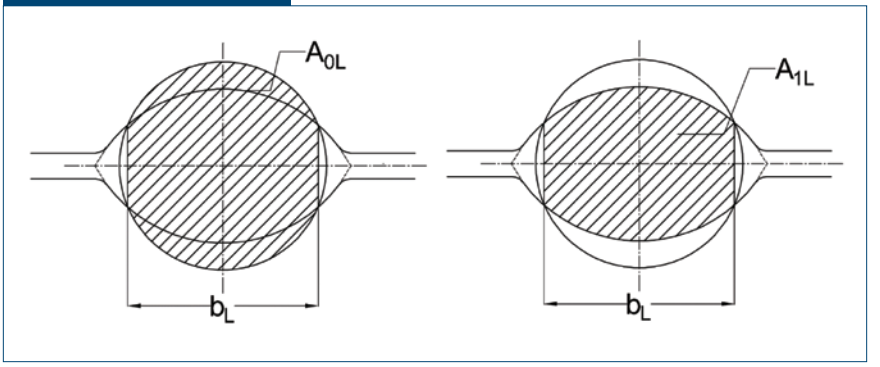

Equivalent Lendl Areas at the pass round to oval.

$$h_{0L} = \frac{A_{0L}}{b_L} \text{ and } h_{1L} = \frac{A_{1L}}{b_L}$$

(Eq. 7)

Additionally, a suitable mean value of the roll diameter in the area of the grooves roll geometry is needed. This working roll diameter can be calculated according to Reference 6:

$$d_w = d_N - h_{1L} + \Delta s$$

(Eq. 8)

In this equation, d_N is the nominal roll diameter, where h_{1L} is given by Eq. 7. Δs subsumes all other effects influencing the roll gap, like elastic stand feedback.

The actual spread is now calculated using Marini's spread (Eq. 7), see Eq. 9.

$$b_1 = b_0 + \frac{2\Delta h b_0 \cdot \left(R - \frac{h_0}{2}\right) \cdot B}{\left(h_1 + b_0 + \frac{b_0\left(h_0 + h_1\right)}{2} \cdot \frac{1+A}{1-A}\right) \cdot \frac{0.91\ \left(b_0\ \ 3h_0\right)}{4h_0} + 2h_1 RB}$$

(Eq. 9)

With the aid values:

$$A = \frac{\sqrt{\Delta h}}{2\mu\sqrt{R}} \text{ and } B = \sqrt{\frac{\Delta h}{R}}$$

(Eq. 10)

Additionally, the spread is influenced by material- and temperature-dependent effects. Recently, a description of these effects as a function of temperature and the chemical composition of the rolled material became possible by construction of an artificial neural network which was trained with experimental data. Details of this analysis can be found in Reference 10.

The models described in the previous sections are now assembled to a fully featured process model for the rolling process in MATLAB. The heart of the model is the geometry calculation. The shapes of the sections and roll grooves are described based on polygonal contours with xy-coordinates of all points. Fig. 2 shows a typical pass with a round entry section (blue), a roll contour (black) and the exit section contour (red).

Here, it can be seen that a portion of the initial cross-section is displaced by the rolls, and another portion reappears due to lateral spread. The final shape of the

Figure 2

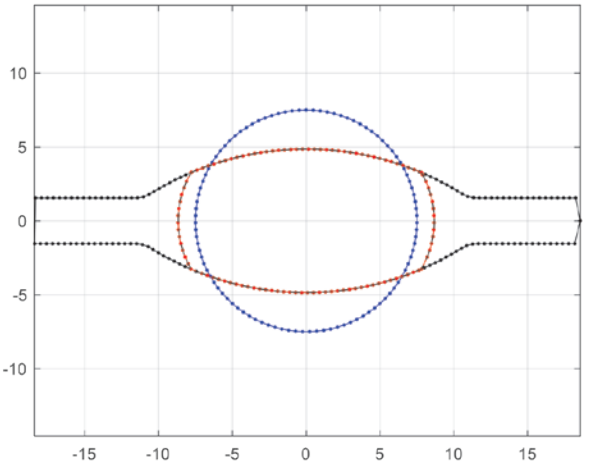

Exemplified calculation of the pass geometry model for a round-oval pass. Initial diameter: 15 mm. Oval height: 9.8 mm.

rolled section is then found as a function of the process parameters and can be used for in-line simulation inside a control model for the rolling process.

Similarly, the underlying models can be applied to the 3-roll and 4-roll rolling processes. Here, a spreading correction must be made to account for the higher elongation efficiency of these processes. Example pass outputs for these processes are shown in Fig. 3.

Figure 3

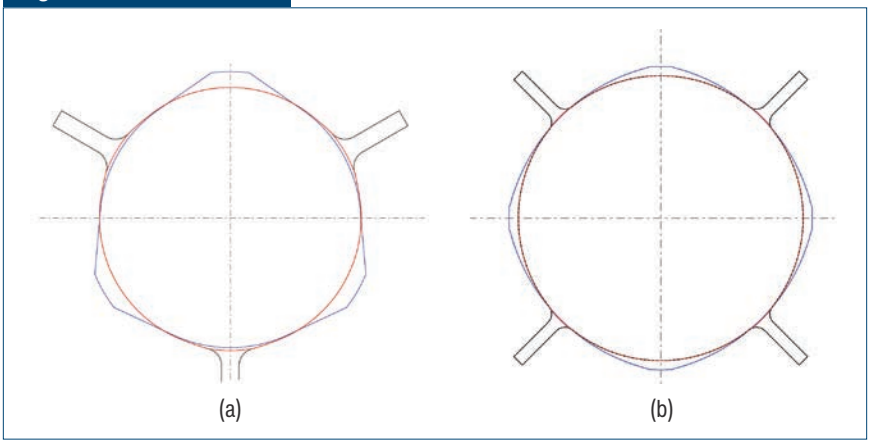

Exemplified calculations for the section shapes in the three-roll process (a) and the four-roll process (b). All three principal rolling process (two, three, and four rolls) for full sections can be handled with the proposed roll gap model.

The Coupling of Multiple Roll Gaps by Interstand Tensions

In Fig. 4, a 3-stand arrangement of a rolling mill is shown exemplarily. The rolls of three subsequent stands rotate at the angular velocities ω_1, ω_2 and ω_3. The backward tension of a stand i will be denoted by $t_{0,i}$, the front tension of stand i will be denoted by $t_{1,i}$.

Generally, the front tension of stand i is equal to the back tension of stand i+1:

$$t_{1,i} = t_{0,i+1} \qquad \text{(Eq. 11)}$$

Figure 4

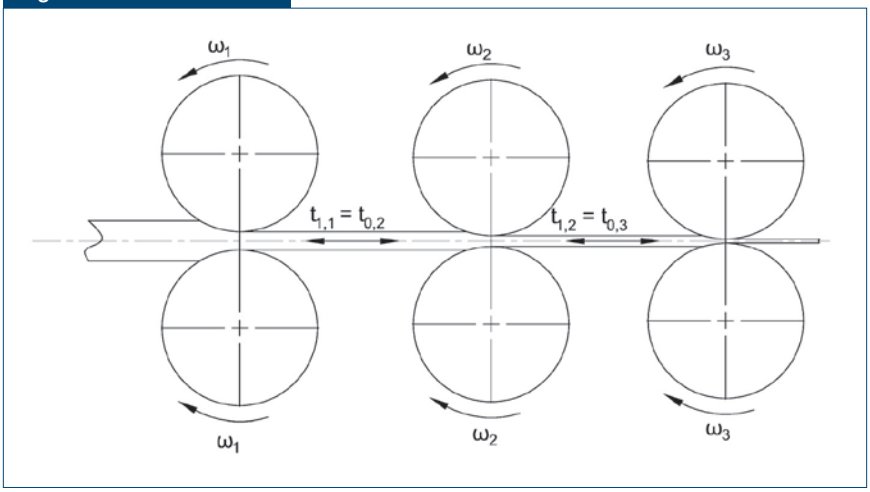

Schematic representation of three subsequent roll gaps in a continuous rolling mill with angular roll velocities and interstand tensions.[12]

As stated above, the tension influences on roll torque and force can be calculated easily using the rolling model. For the direct tension influence on spread, an additional empirical model must be employed. Mauk provided a framework for the tension influenced additional deformation in 1999,[13] given in Eq. 4.

$$\varphi_{tot} = \varphi_0 + \Delta\varphi_\sigma \qquad \text{(Eq. 12)}$$

Here, φ_0 is the calculated true strain of the pass without tensions. The tension influence term $\Delta\varphi_\sigma$ is a function of the front and back tension and the geometric properties of the rolling pass. Note that the influence of the back tension is higher than that of the front tension.[13]

Being able to assess the interstand tension stresses acting in a rolling process is of great importance for the construction of the underlying metal forming part of the control model, but the tension influences are very non-linear and influence several stands at the same time. For simpler cases (that is, without a tension-dependent spread), a linearized model for the interstand tension assessment can be constructed with good success, but the linearization breaks down for the highly non-linear spread influences which are faced in the section rolling case. To enable a backward calculation of the acting interstand tensions from the rolling parameters (i.e., the measured roll and material speeds and section shapes), either a time-consuming iterative procedure must be applied to solve the non-linear system of multiple coupled roll gaps, or a data-driven modeling of the relationship between N roll speeds and (N-1) tensions between the N roll gaps must be carried out. In the present case, the data-driven modeling was

Figure 5

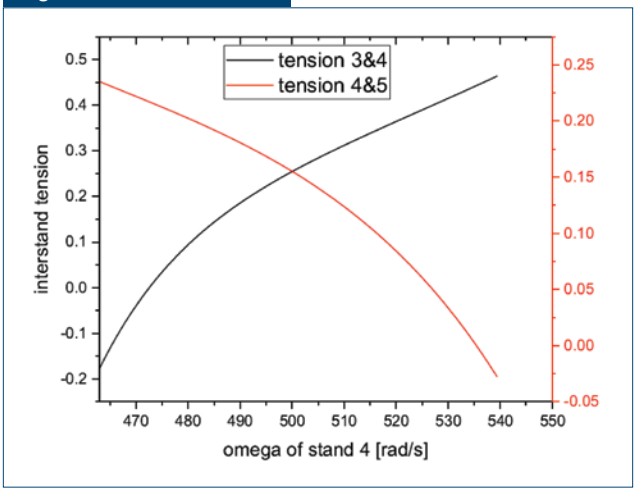

Reaction of related interstand tensions in a continuous rolling mill to variations of the roll speed of one mill stand.[14]

applied, which resulted in a fast model for computation of the present interstand tensions during the rolling process of long products.

Fig. 5 shows a calculated result for this model for a 6-stand rolling block in an industrial wire rod mill. On the vertical axes, the interstand tension is shown in relation to the mean flow stress.

In this computational example, the angular roll velocities of stands 3 and 5 remain constant, where the roll velocity of stand 4 is varied. It can be seen from these results that the back tension of stand 4 (or tension between stands 3 and 4) increases when the roll speed of stand 4 is increased. At the same time, the front tension of stand 4 (or tension between stands 4 and 5) decreases with increasing roll speed. This data already accounts for the spread-reducing effect of the tensions and the influence of the tensions on the global volume flux of the rolling process.

The indirect measurement of acting interstand tension stresses is one important task of the control model, and this aim can be reached with a combination of analytical and data-driven modeling as described here. Another task is the prediction of variations in the rolling parameters that need to be realized to achieve variations in the interstand tension (to increase or decrease the tension). This is especially important for the present task of controlling the rolling process.

Figure 6

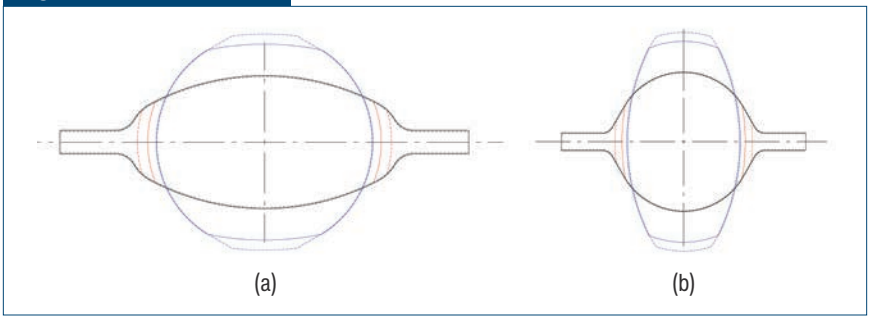

Influencing method of the section shape by means of interstand tensions. Solid lines: with elastic stand deformation and interstand tensions. Dashed lines: with rigid stands and the tension-free case.

It has been observed that lateral spread can be influenced effectively by means of the interstand tension. If too much spread is reported by the QFM sensor, the tension should be temporarily increased to decrease the width of the rolled section. Tension can be increased or decreased by influencing the velocity mismatch between two subsequent mill stands. The necessary roll speed variation can be calculated by the present model. Fig. 6 shows two examples with predicted section shapes.

The dashed lines in Fig. 6 correspond to the case without tensions and without elastic rolling stand deformation. In the solid lines, elastic rolling stand deformation is considered along with a uniform interstand tension of 20% of the material's flow stress between each two subsequent rolling stands. In Fig. 6a, the oval pass is shown, and Fig. 6b the next pass oval to round. The section evolution is interconnected between the two passes because the varied section height from the oval pass serves as the initial width for the round pass.

Figure 7

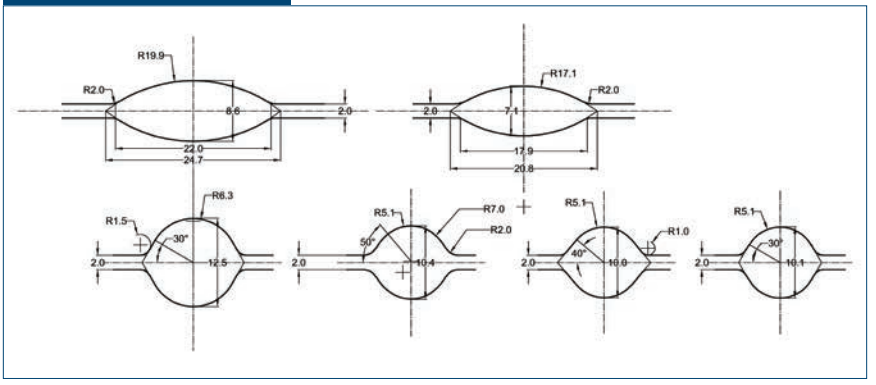

Pass design of the laboratory mill at the University of Duisburg-Essen (UDE).

On the other hand, the exit width of the oval pass is the entry height for the round pass.

The elastic rolling stand deformation does not lead to a huge increase of section height, and one should also keep in mind that the rolling force is reduced by the tension, leading to a lower elastic feedback of the roll gap. In contrast to this, the tension influence on the spread is obvious. In both passes, oval and round, the spread is reduced quite extensively due to the 20% of interstand tensions. Because of this strong influence, interstand tensions can be used effectively to counteract an overspreading of the sections.

Rolling Trials Carried Out at the University of Duisburg-Essen

At the metal forming lab at UDE, rolling trials were conducted to validate the model and to examine the velocity and material flow pattern of the rolling process. For this purpose, a pass design was worked out for an initial round section of 15 mm, as shown in Fig. 7.

The 15-mm round entry section would be deformed in two passes to an intermediate round section of 12.5 mm, and in two further passes into a finishing round section of 10 mm. Fig. 8 shows the laboratory rolling mill used for the trials. It is equipped with measurement sensors for entry and exit temperature, velocity, angular roll speed, as well as exit section height and width. The rolls with the pass design shown in Fig. 7 have a nominal diameter (at the roll gap) of 208 mm.

During the passes, roll force, torque, as well as the exit and entry velocities of the rolled bar were measured. Comparisons between calculated and measured roll forces were carried out systematically, giving results in close agreement.

From the equations of the rolling model as well as the spread calculation, it is evident that the coefficient of friction plays a great role in the accurate modeling of rolling process and the creation of a digital process twin. Therefore, investigations were undertaken to measure the coefficient of friction without any special equipment which would prevent a normal rolling operation.

It is clear that the volume flux of the rolling process is a constant with respect to time:

$$A \cdot \nu = const \Rightarrow A(\alpha_N) \cdot \nu_R \cos(\alpha_N) - A_1 \nu_1 = 0$$

(Eq. 13)

Based on this equation, one can find a relationship between the forward slip and the neutral angle:

$$\kappa = \frac{\nu_1 - \nu_R}{\nu_R} = 1 - \frac{A_N}{A_1} \cdot \cos\alpha_N$$

(Eq. 14)

The cross-section at the neutral angle A_N must be again expressed by the geometry:

$$A_N = A(\alpha_N) = h(\alpha_N) \cdot b(\alpha_N)$$

(Eq. 15)

Figure 8

(a) (b)

Laboratory rolling mill at the metal forming lab of UDE: operator side view (a) and entry side view (b).

Figure 9

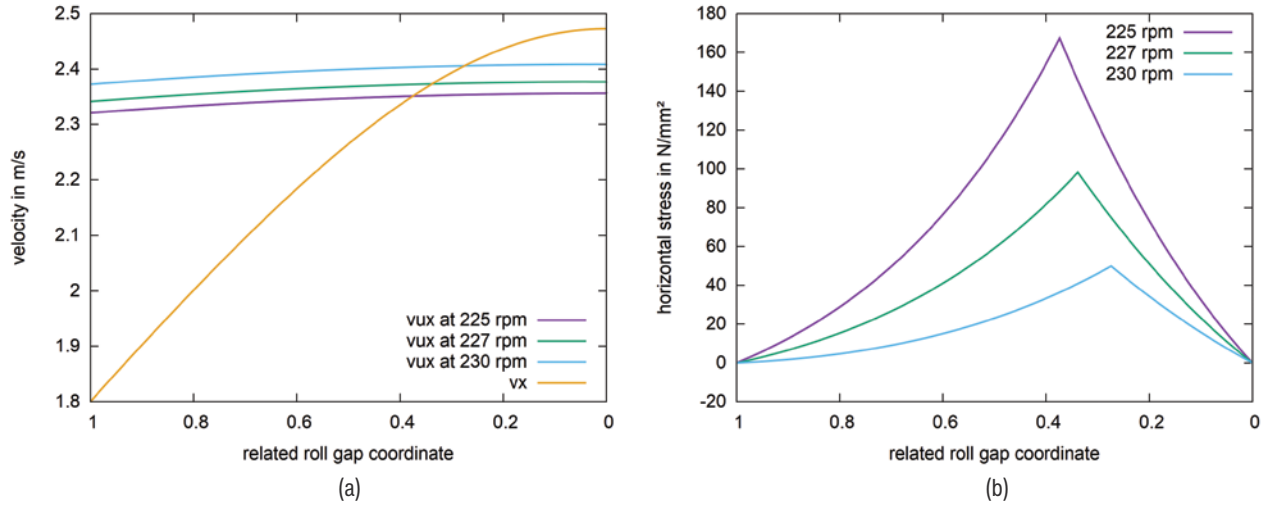

Velocity distribution (a) and stress distribution (b) for different roll velocities at a constant volume flux.

Introducing the roll gap width and height functions, Eq. 14 gets non-linear and must be solved numerically to yield the neutral angle, which is connected to a certain measured forward slip. Once the neutral point of the rolling process is known, a numerical reverse evaluation of the roll gap is carried out to find the corresponding coefficient of friction.

Fig. 9a shows the horizontal material velocity distribution v_x in the roll gap for an exemplified flat pass (yellow line). The horizontal roll surface velocities v_{ux} are shown for three different rotational speeds of the rolls. It can be seen that the intersection point of these curves with the v_x-curve are different for each roll velocity, therefore yielding different neutral angles.

In Fig. 9b, the associated horizontal stress distributions are represented. As there is a unique relationship between the coefficient of friction and the neutral point, one can identify the coefficient of friction from the forward slip measurement through adaption with the rolling model. Apparently, a more sophisticated rolling model must be used not relying on constant sticking friction throughout the roll gap. The latter simplification is present in all simple analytical hot rolling models. The non-simplified version of Alexander's rolling model is used, as given by Eqs. 2 and 3.

Table 1 shows a summary of the data of the considered roll passes. For these data, the related neutral angles were found numerically according to Eq. 1 and attained values between 0.275 and 0.375, which are just typical data for hot rolling. The friction coefficient range between 0.186 and 0.373 for the considered pass data.

While Fig. 9 gives a general example for the process of friction measurement in a flat pass, an example for actual measurements of forward slip and friction at a hot rolling round-oval pass is presented. Fig. 10 shows the actual pass geometry for a rolled oval section, while Table 2 gives an overview of the data that where measured and determined for this pass.

From the measured entry and exit velocities as well as the roll velocity, a forward slip value of 3.07% was calculated. This provided a related neutral angle of β_N = 0.3104. The numerical adaption of Alexander's rolling model resulted in a forward slip-equivalent

Table 1

Evaluation Data of the Roll Passes Shown in Fig. 9

Entry height h_0 in mm	Exit height h_1 in mm	Initial width b_0 in mm	Final width b_1 in mm	Entry velocity v_0 in m/s	Rotational roll speed n in rpm	Forward slip κ	Related neutral angle β_N	Friction coefficient μ
10	7	50	52	1.8	230	2.66 %	0.275	0.186
10	7	50	52	1.8	227	4.013 %	0.338	0.271
10	7	50	52	1.8	225	4.937 %	0.375	0.373

Figure 10

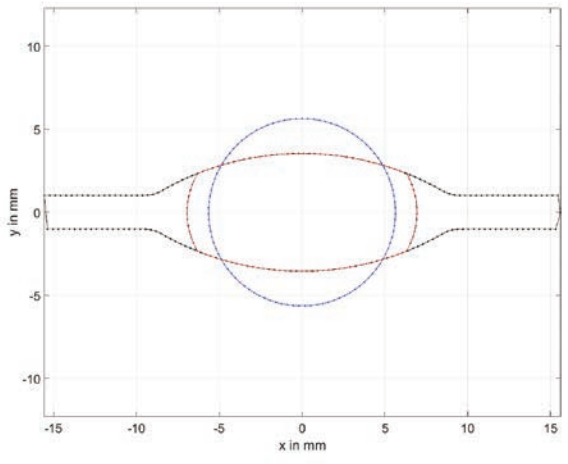

Actual pass geometry of the section for which the friction evaluation was carried out. For an overview of data, see Table 2.

friction coefficient of $\mu = 0.252$. This value is relatively low for a hot rolling case, which can be attributed to the clean laboratory environment with freshly grinded rolls under which the trial was undertaken.

The friction assessment by means of forward slip measurements was reported before for flat rolling,[16] but the present approach seems to be the first successful friction measurement under hot rolling conditions of a non-flat cross-section with extra difficulties due the non-negligible lateral spread.

Model Processing of In-Line Measurements From the Mill

The QFM cross-section sensor as shown in Fig. 11 returns the cross-section in mm^2 at the measurement position. For a precise evaluation, width and height effects must be distinguished from each other, because from an integral cross-sectional variation in mm^2, it cannot be determined if it is due to a height or width fault. These fault types require different methods of counteraction.

The pass geometry model described can be used to segregate the height effects from the width effects. With the help of the model, one can calculate the material cross-section for a specific groove geometry as a function of the roll gap screwdown and the section width. A backward analysis of this relationship yields the unknown section width when the cross-section and the roll gap were measured. To benefit from this technique, an independent continuous measurement of the roll gap is needed additionally.

The synthetic data generated by the pass geometry model was used to train an artificial neural network which can be used for the backward calculation. Fig. 12c shows the interdependency of cross-section, roll gap and section width for the oval roll contour shown in Fig. 2, while Fig. 12a and 12b show much different oval section shapes, rolled from the same groove and same entry section, depending on roll gap setting and material- and temperature-dependent spreading behavior of the rolled material. These section shapes can be concluded from the roll gap and cross-section measurements as described above.

The material- and temperature-dependent spreading behavior of the rolled materials is described with a neural network, based on data of flat rolling trials with different steel materials and a temperature range between 800°C and 1,200°C taken from Grosse and Gottwald,[6] where the temperature and the chemical composition of the specific steel material were used as input parameters for the neural network.

Discussion

In the research project PIREF, the authors were able to develop a model for hot rolling of full sections which can be used in a control model for the rolling process.

Table 2

Exemplarily Measured Data in a Round-Oval Pass

Initial diameter d_0 in mm	Exit width b_1 in mm	Exit height h_1 in mm	Entry velocity v_0 in m/s	Exit velocity v_1 in m/s	Forward slip κ	Related neutral angle β_N	Friction coefficient μ
11.28 mm	13.88	7.08	0.3046	0.3621	3.07 %	0.3104	0.252

Figure 11

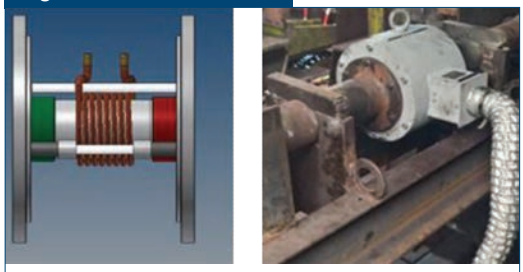

QFM cross-section sensor: schematic drawing (a) and in industrial application (b).[15]

Figure 12

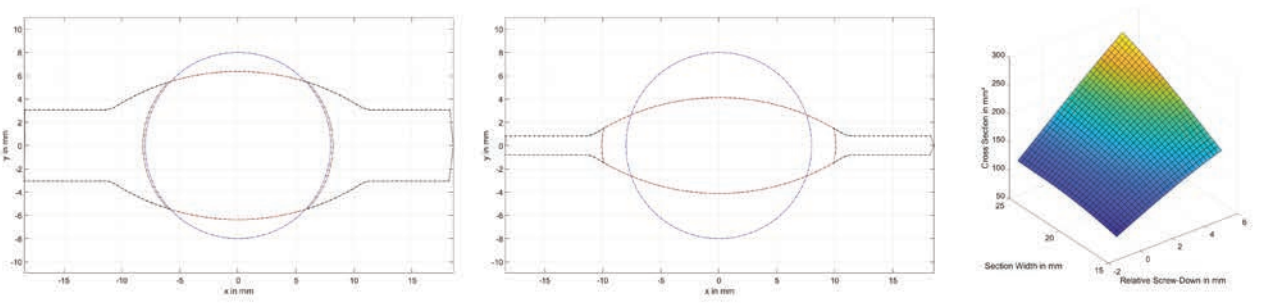

Different cross-sections from the same roll contour: wide opened gap, low spread (a); closed gap, higher spread (b); data for relationship between roll gap, section width and cross-section (c).

This article presented a method that allows the actual section shape to be deduced from measured cross-section and roll gap screwdown. This allows the cross-sectional variations to be decomposed in height- and width-affecting parameters and therefore the initiation of suitable counteracting measures. The theoretical basis was built for an active tension control in rolling of full sections. This is accomplished by an on-line enforcement of the interstand tensions by continuous measurement of roll and material velocities. As some of the submodels are too sophisticated to be evaluated on-line in a numerical way, they were cast into data-driven models using machine-learning techniques with synthetic data. A method for on-line evaluation of the coefficient of friction was presented with a specific application to full section rolling. In the future, the validity range of the model shall be extended. For this purpose, more rolling trials must be carried out to gather data to be fed into the empirical data-driven model for the interstand tension influence on spread, which is a central feature of the current model. In the foreseeable future, the overall control model should be implemented in an industrial rolling mill for a test run.

Acknowledgments

The authors thank the European Regional Development Fund for providing funding of the research project PIREF under project code EFRE-0800805. Special thanks are owed to project partners representing the University of Siegen, the University of Applied Sciences Ruhr-West, EMG Automation GmbH and SMS group GmbH for the fruitful discussions which led to the developments presented in this article.

References

1. T. von Karman, *Z. Ang. Math. Mech.,* 1925, pp. 139–141.
2. P.J. Mauk and R. Kopp, "Spread Under Hot Rolling," *Der Kalibreur,* Vol. 37, 1982, pp. 3–55.
3. J.M. Alexander, "On the Theory of Rolling," *Proc. R. Soc.,* Vol. 326, No. 1567, 1972, pp. 535–563, DOI: 10.1098/rspa.1972.0025.
4. J.H. Hitchcock, ASME Report of Special Research Committee on Roll Neck Bearings, 1935.
5. A.E. Lendl, "Rolled Bars, Calculation of Spread Between Non-Parallel Roll Surfaces," *Iron and Steel,* September 1948, pp. 397–402.
6. C. Overhagen, Ph.D. Eng. dissertation, University of Duisburg-Essen, 2018.
7. N. Marini, "New Lamination Theory," (in Italian) *La Metallurgia Italiana,* 1941, pp. 292–309.
8. C. Overhagen and P.J. Mauk, "Flexible Groove Sequences for Hot Rolling a Number of Materials," *AISTech 2012 Conference Proceedings,* 2012.
9. W. Grosse and H. Gottwald, "The Influence of Carbon, Manganese, Chromium, Nickel and Molybdenum on the Free Spreading of Steels," *Stahl und Eisen,* Vol. 79, No. 12, 1959, pp. 855–866.
10. M.T. Gruszka and C. Overhagen, "Predicting Material and Temperature Dependent Spreading Behaviour of Steel Materials for Hot Rolling of Round Sections Using an Artificial Neural Network," *12th International Rolling Conference,* Trieste, Italy, 2022.
11. C. Overhagen, "Pass Design Methods for Three- and Four-Roll Rolling Processes – Comparison and Analysis," *11th International Rolling Conference,* Sao Paulo, Brazil, 2019.
12. C. Overhagen, "Numerical Assessment of Interstand Tensions in Continuous Hot Rolling Processes of Flat and Long Products," *Int. J. Adv. Manuf. Technol.* 127, 2023, pp. 4677–4696, https://doi.org/10.1007/s00170-023-11584-x.
13. P.J. Mauk, "Analysis of Interacting Influence Parameters on the Tolerances of Wire Rod and Bars in the Rolling Process," *6th ICTP International Conference on Technology of Plasticity, Erlangen,* 1999.
14. Y. Yang, "A Data-Driven Model for Interstand Tensions in Wire Rod Finishing Blocks Based on Analytical Computations," M.Sc. thesis, University of Duisburg-Essen, 2020.
15. EMG Automation GmbH, https://www.emg.elexis.group.
16. W.Y.D. Yuen, "Determination of Friction From Measured Forward Slip and Its Applications in Hot Strip Rolling," *First Australasian Congress on Applied Mechanics,* February 1996. ✦

This paper was presented at AISTech 2023 – The Iron & Steel Technology Conference and Exposition, Detroit, Mich., USA, and published in the AISTech 2023 Conference Proceedings.